All order moments and other functionals of the increments of some non-Markovian processes

Journal of Statistical Mechanics: Theory and Experiment
An IOP and SISSA journal

All order moments and other functionals of the increments of some non-Markovian processes

Marie-Christine Néel[1], Solonjaka Hiarinstoa Rakotonasy[1], Daniela Bauer[2], Maminirina Joelson[1] and Marc Fleury[2]

[1] Université d'Avignon et des Pays de Vaucluse, UMR 1114 EMMAH, 84018 Avignon Cedex, France
[2] IFP Energies nouvelles, 1 et 4, avenue de Bois Préau 92852—Rueil-Malmaison, France
E-mail: mcneel@avignon.inra.fr, Solonjaka-Hiarintsoa.Rakotonasy@avignon.inra.fr, daniela.bauer@ifpenergiesnouvelles.fr, maminirina.joelson@univ-avignon.fr and marc.fleury@ifpenergiesnouvelles.fr

Received 26 October 2010
Accepted 6 January 2011
Published 1 February 2011

Online at stacks.iop.org/JSTAT/2011/P02006
doi:10.1088/1742-5468/2011/02/P02006

Abstract. We propose a theoretical framework to analyze nuclear magnetic resonance (NMR) experiments for the description of dispersion processes featuring memory effects. Memory effects, addressed here, can be represented by subordinated Brownian motions with random time changes that invert Lévy time processes, with stable densities of exponent between 0 and 1. According to whether the Lévy process has a drift equal to zero or not, the subordinated motion has a p.d.f that solves the fractional Fokker–Planck equation or the fractal mobile/immobile model. NMR experiments can measure the characteristic function of displacements of water molecules and facilitate their interpretation in media showing memory effects. We give mathematical expressions for the moments and averaged exponentials of the increment of subordinated Brownian motions within the framework of fractal MIM and FFPE. The results are illustrated on the basis of a numerical method.

Keywords: stochastic particle dynamics (theory), stochastic processes (theory), stochastic processes (experiment), transport properties (theory)

1742-5468/11/P02006+18$33.00

Contents

1. Introduction

In addition to the probability density function (p.d.f) commonly used to represent the concentration of a solute, different types of functionals of random processes describing dispersion have been addressed in the past. Such functionals may be moments and also path integrals [1] representing various observables attached to trajectories of tracer particles. The statistics of such observables, among which we find occupation times, has been the subject of theoretical work reviewed in [1] and mentioned in the textbooks [2, 3]. All of this work was achieved within the Markovian context, in which multi-point p.d.f.s can be split into products of one-point p.d.f.s. However, recent approaches deal with non-Markovian processes, applicable to mass transport with memory effects [4]–[9]. Interestingly, p.d.f.s of walker displacements can be measured in nuclear magnetic resonance (NMR) velocimetry experiments, and this is the motivation to develop specific functionals and moments of the increments of some transport processes involving stagnation periods, associated with memory effects.

The memory effects, addressed here, are marked by data indicating that a fraction of a solute may be retained for abnormally long times. This is observed for example on break-through curves (BTC) describing the concentration of a solute versus time at the outlet face of partially saturated sand columns [10]. Such curves can be modeled at long times by power laws and indicate a failure of Fick's law. It suggests that certain tools, commonly used for data processing based upon the Markov property, are inappropriate. In other words, predicting the future of a system showing such effects,

doi:10.1088/1742-5468/2011/02/P02006

J. Stat. Mech. (2011) P02006

on the basis of its description at a given instant, may be hazardous. A promising approach to such situations consists in representing small scale motions of walkers by means of random processes, whose (one-time) probability density function satisfies the fractal mobile–immobile model (MIM) [12, 11, 13]. This equation generalizes Fourier's law, that rules the density of Brownian motion, and is very similar to the fractional Fokker–Planck equation (FFPE) [14]–[22]. Both equations contain integro-differential operators of fractional orders, and have solutions that ultimately decrease slowly (as a power of time). The first difference, between the approaches, is a time derivative of the order of one in the fractal MIM (and not in the FFPE), resulting in almost a Fickian behavior at early times, similarly to what is observed in many porous media [23]. A consequence is that solutions of both equations are very similar at late times, and significantly differ at early times. The fractal MIM is apparently more appropriate than the FFPE for transport in porous media. Comparing such equations with concentration profiles of an injected solute allows one to evaluate an adequate model for solute spreading in space and time. An alternate and complementary experimental approach is to use NMR velocimetry to investigate fluid motions without the need for a tracer. These methods have been known for a long time [24] and have been used to study dispersion [25, 26] in the framework of the so-called propagator formalism. Again, this formalism can also be questioned when non-Markovian processes have to be considered, because memory effects are suspected to occur. In the NMR context, the joint statistics of molecule positions at more than one time is the key aspect and, for memory effects, the adequate description of stagnation periods is central. For processes corresponding to the FFPE, multi-time p.d.f.s were communicated by [5] and [7], including expressions for low order moments. In fact, all moments of the increments of inverse subordinators of Lévy processes are given at the same time by a general formula [27].

In this paper, we derive theoretical and numerical tools to analyze transport experiments using NMR techniques, and the major concern of this work is to include memory effects observed in unsaturated porous media [10]. Without disregarding the FFPE that has been extensively studied, we focus on the fractal MIM, a variant of the mobile–immobile model [28], used for three decades to study convection and dispersion in porous media, particularly in the environment. The original MIM describes the transport of a solute in media where immobile steps as well as displacements can be represented on comparable timescales. However, it does not include BTC decreases following powers of time, as observed in unsaturated columns. Such features are better described by a fractal variant of MIM introduced by [12] after a previous attempt by [29]. The more general variant, also referred to as fractal MIM, is the macroscopic version of stochastic models for individual motions of fluid parcels or tracer particles [13], [30]–[32], combining Brownian motion in a uniform velocity field, and immobile periods of random durations, the latter being distributed by a Lévy law [33]–[35].

The above mentioned general formula for moments applies to such models. Hence, considering, in particular, models associated with the fractal MIM, we propose mathematical expressions for all moments of walker displacements. Low order moments of (one-time) positions of walkers were computed by [11]. From the complete sequence of all order moments of the displacement, we will derive the mathematical expectation of its exponential. A non-local operator, introduced in [31] and [32], in view of numerical computations, will provide additional help. We will also show similar results for the

J. Stat. Mech. (2011) P02006

extensively studied [5, 19, 20] subordinated Brownian motion (SBM), which corresponds to the FFPE.

The structure of the paper is as follows. We will first recall the connection between the fractal MIM and stochastic processes, based upon Brownian motion subordinated by an increasing time process (section 2). Section 3 will be devoted to the moments of the increments (at all orders) of the inverse subordinator, from which we will deduce those of the individual displacements of walkers representing fluid particles. Theoretical issues will be illustrated by numerical comparisons with Monte Carlo simulations. Then, in section 4, we will pass to the mathematical expectation of the displacement exponential (namely, the characteristic function). Within the context of the FFPE, the same approach yields simpler computations that will be outlined at each step. We will thus retrieve and extend previously existing results.

2. A process for mass transport with immobile periods

The fractal MIM [12] reproduces both heavy-tailed BTC, and Fickian behaviors [11, 12, 31], observed at early times. It also rules the evolution of the p.d.f. of a variant of the subordinated Brownian motion that combines two essential components, namely Brownian motion itself and a subordinator that needs to be accurately set. As Brownian motion, subordinated Brownian motions are efficiently approximated by random walks [11, 13, 19].

2.1. Random walks with immobile periods, and the diffusive limit

A natural and simple one-dimensional random process $x^\tau(t)$, combining advection and dispersion with immobile periods, is given by the following random walk (started from x_0 at time $t = 0$)

$$x_{n+1} = x_n + v\tau + \sqrt{2D\tau}N_n \tag{1a}$$

$$t_{n+1} = t_n + \tau + \tau^{1/\gamma}W_n. \tag{1b}$$

Individual trajectories are piecewise linear, and join the sequences of points (x_n, t_n), $(x_n + v\tau, t_n + \tau)$, $(x_{n+1}, t_n + \tau)$ and (x_{n+1}, t_{n+1}). The time that a tagged walker spent moving, called the operational time [36], increases between t_n and $t_n + \tau$ only. Hence, piecewise linear curves joining sequences $(n\tau, t_n)$ compute the physical (or total) time from the operational time [11]. Note that between two successive immobile periods $\tau^{1/\gamma}W_n$, there is always a well-separated time step τ, devoted to a displacement of amplitude $v\tau + \sqrt{2D\tau}N_n$. This displacement is due to the average flow field v and to dispersion, even if v is equal to zero. Here, N_n and W_n are random numbers, τ is a timescale, the diffusivity D and the averaged flow v are assumed constant. To be more precise, N_n are identically distributed random Gaussian numbers with zero mean and unit variance. The W_n are (also identical) positively valued Lévy stable random variables of exponent γ, all variables being independent of each other. Notice that Lévy laws, supported by R^+, only exist for $\gamma \leq 1$, and that the limiting case $\gamma = 1$ corresponds to the deterministic situation where the W_n become Dirac atoms [37]. For $\gamma < 1$, the Laplace transform of the density of the W_n is $\mathrm{e}^{-\Lambda\lambda^\gamma}$, with λ representing the Laplace variable while Λ is a positive scaling factor. At large values of t, the p.d.f. of the random variable W_1

J. Stat. Mech. (2011) P02006

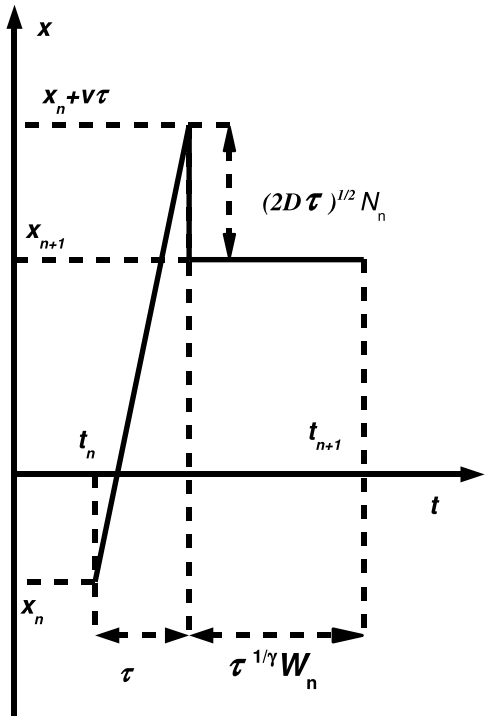

Figure 1. A step of the random walk described by equations (1), allowing a tagged walker to move from x_n to $x_n + v\tau$, and then to x_{n+1} between t_n and $t_n + \tau$ (sub-step 1) and after that to remain immobile until time t_{n+1} (sub-step 2). Motion is restricted to sub-step 1, and entails an instantaneous random jump of amplitude $\sqrt{2D\tau}N_n$, occurring at the end of a convective displacement of amplitude $v\tau$, itself representing the influence of the average velocity field.

becomes $\Lambda(t^{-\gamma-1}/|\Gamma(-\gamma)|)$. Hence, γ weights the heterogeneity of the stagnation periods, whose intensity is represented by Λ. Random walks as given in equations (1) accumulate successive independent steps, each of them allowing a tagged walker to pass from its position x_n at time t_n to its position x_{n+1} at time t_{n+1}. As illustrated in figure 1, each of these steps splits into two sub-steps, which are (1) a period of duration τ where each walker moves over a distance of $v\tau+\sqrt{2D\tau}N_n$ and (2) a random immobile stay of duration $\tau^{1/\gamma}W_n$. Figure 2 shows trajectories (with many steps) for three values of γ, that are 0.5, 0.8 and 1.

Straightforward application of the reasoning of [19] and [30] shows that in the limit $\tau \to 0$, $x^\tau(t)$ tends to $x(t)$ as

$$x(t) = x_0 + vZ(t) + \sqrt{2D}B(Z(t)) \tag{2}$$

where B represents standard Brownian motion, while $Z(t)$ is the increasing time increment that inverts the (also increasing) 'direct' process $U(z) = z + U_{\mathrm{FFPE}}(z)$, i.e.

$$Z(t) = \inf\{z \in R^+ / U(z) > t\}. \tag{3}$$

Here, $U_{\mathrm{FFPE}}(z)$ is a strictly stable Lévy process [30] all of whose finite-dimensional distributions are equal to that of $z^{1/\gamma}W_1$. The process $Z(t)$, inverting U, computes the 'operational time' corresponding to the physical time t [36, 38], i.e. the time periods during

J. Stat. Mech. (2011) P02006

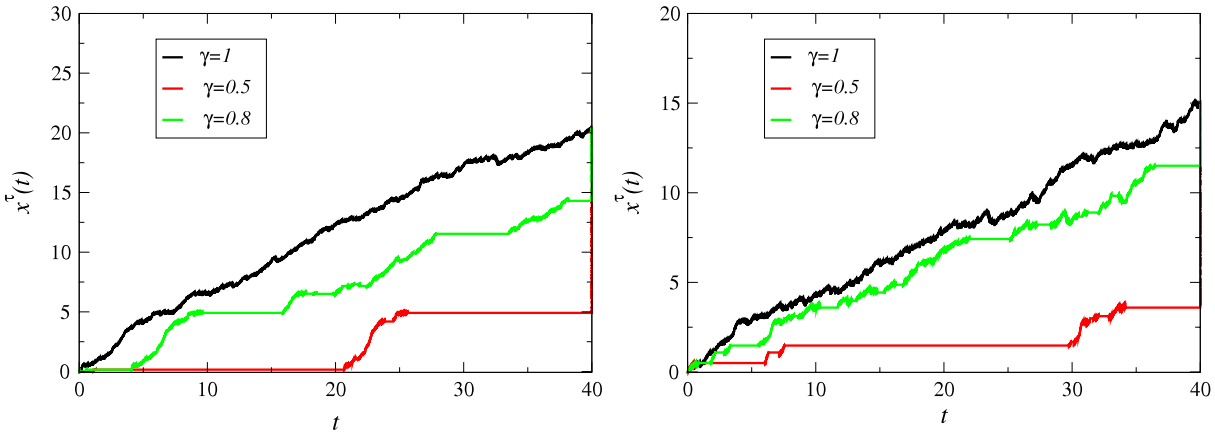

Figure 2. Some trajectories of $x^\tau(t)$ for $\tau = 0.01$, $\gamma = 0.5$, $\gamma = 0.8$ and $\gamma = 1$. The right side of the figure displays trajectories, all obtained from a given sample $N_1, \ldots, N_n \ldots$ and corresponding to different values of γ. The left side corresponds to another sample $N_1, \ldots, N_n \ldots$. All of them correspond to $D = 0.1$, $\Lambda = 1$, and $v = 1$. For $\gamma < 1$, walkers sometimes stay immobile for long periods, less marked when γ is increased. For $\gamma = 1$, differently, trapping durations have a finite average, equal to the time spent moving, multiplied by Λ: diffusion becomes normal.

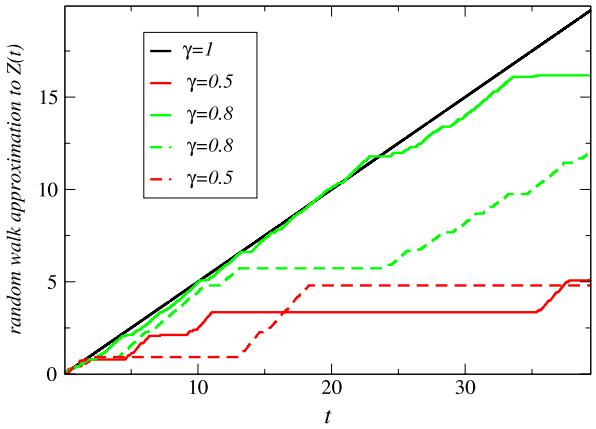

Figure 3. Approximate trajectories of $Z(t)$, for three values of γ and the same value of Λ. Full and dashed lines of a given color represent two sample paths of the same process $Z(t)$, i.e. correspond to the same value of γ.

which there is no motion are not taken into account. In the limiting case $\gamma = 1$, with $Z(t) = t/(1+\Lambda)$, the process $x(t)$ becomes the uniformly retarded Brownian motion $x_0 + vt/(1+\Lambda) + \sqrt{2D}B(t/(1+\Lambda))$ in a constant velocity field. An important point is that $B(Z(t))$ is independent of $Z(t)$ [20]. Since piecewise linear curves joining sequences $(n\tau, t_n)$ approximate trajectories of the direct process $U(z)$, joining the $(t_n, n\tau)$ approximates the sample paths of the inverse process $Z(t)$ [11], as displayed on figure 3.

J. Stat. Mech. (2011) P02006

From the point of view of the fractal MIM, in the limit $\tau \to 0$ [13, 30, 32], the random walk $x^\tau(t)$ tends to a limit whose p.d.f. $P(x,t)$ satisfies the following equation

$$\partial_t P = \partial_x[\partial_x D(\mathrm{Id} + \Lambda I_{0,+}^{1-\gamma})^{-1} P - v(\mathrm{Id} + \Lambda I_{0,+}^{1-\gamma})^{-1} P]. \tag{4}$$

Here Id denotes the identity operator, and the non-local in time operator $(\mathrm{Id}+\Lambda I_{0,+}^{1-\gamma})^{-1}$ is the inverse of the (also non-local in time) mapping $\mathrm{Id}+\Lambda I_{0,+}^{1-\gamma}$, where $I_{0,+}^{1-\gamma}$ is the fractional integral of order $1-\gamma$ (its definition [39, 40] is recalled the appendix). In equation (4), $(\mathrm{Id}+\Lambda I_{0,+}^{1-\gamma})^{-1}P(x,t)$ represents the density of mobile particles at point x, at time t [31, 32]. For $\gamma = 1$, the mapping $\mathrm{Id} + \Lambda I_{0,+}^{1-\gamma}$ reduces to a multiplication, and equation (4) becomes the MIM [28] with a retardation factor of Λ.

The fractional advection dispersion equation, which coincides with the FFPE when all parameters are constant, has been extensively studied [14]–[17]. It is given by

$$\partial_t P = \Lambda^{-1} D_{0,+}^{1-\gamma} \partial_x [\partial_x DP - vP], \tag{5}$$

with three independent parameters $\gamma, v\Lambda^{-1}$ and $D\Lambda^{-1}$. This equation governs the p.d.f. of the hydrodynamic limit of random walks passing through points (x_n, T_n) satisfying (1*a*), with $T_{n+1} = T_n + \tau^{1/\gamma} W_n$ instead of (1*b*) [11]. The amplitude of the displacement $v\tau + \sqrt{2D\tau}N_n$ and the time span $\tau^{1/\gamma}W_n$ are prescribed, but there are no separate time steps for motion and trapping. Moreover, the random time $T_{n+1} - T_n$ may be very long, or also sometimes almost equal to zero, differently from what we noticed for (1).

Since the Riemann–Liouville derivative $D_{0,+}^{1-\gamma}$ is the left inverse of the integral $I_{0,+}^{1-\gamma}$, we recognize in equation (5) a partial differential equation (p.d.e) very similar to equation (4), except that the mapping $(\mathrm{Id}+\Lambda I_{0,+}^{1-\gamma})^{-1}$ has been replaced by the left inverse of $(\Lambda I_{0,+}^{1-\gamma})$. Solutions to equations (4) and (5) tend to behave similarly at large values of t. Nevertheless, significant differences are observed at finite values of t: when t is small, solutions to (4) resemble that of Fourier's law, itself obtained from (4) by setting $\Lambda = 0$.

The passage to the limit $\tau \to 0$, introduced above for the fractal MIM, was applied by [19, 30, 38] to the FFPE (5). This latter equation represents the evolution of the p.d.f. of processes, as given by equation (2), except the fact that the operational time is the inverse of another subordinator [19, 30, 38], namely $U_{\mathrm{FFPE}}(z)$ itself. To avoid mismatches, similar symbols will be used for all processes (such as Z, x, U) and functions corresponding to this case, denoted by the subscript 'FFPE'. They correspond to the operational time $Z_{\mathrm{FFPE}}(t)$ that inverts $U_{\mathrm{FFPE}}(z)$ (whose finite-dimensional marginal distributions are that of $z^{1/\gamma}W_1$). Equation (5) represents the density of the process $x_{\mathrm{FFPE}}(t) = x_0 + vZ_{\mathrm{FFPE}}(t) + \sqrt{2D}B(Z_{\mathrm{FFPE}}(t))$. The self-affine process $B(Z_{\mathrm{FFPE}}(t))$ [30] has a considerable importance, especially in view of diffusion on fractals, but it is likely that the fractal MIM (with four parameters (D, v, Λ, γ) instead of three for FFPE) [23] is better suited for mass transport in porous media [12, 11, 13].

In this work, we focus on both models, however the fractal MIM requires considerably more attention. This is due to the fact that results of the FFPE have simpler expressions, and are sometimes already available in the literature.

2.2. Displacements of $x(t)$, and relation to NMR experiments

In tracer experiments, concentration profiles and BTC are measured after some solute has been injected in a porous medium. This type of experiment can be interpreted

J. Stat. Mech. (2011) P02006

using equation (4), a very useful tool together with the study of moments for inverting parameters [11]. However, it cannot be used to interpret NMR experiments that measure a signal related to the displacement of walkers in the entire porous volume without the need of using a tracer. In such experiments, a time-varying gradient of magnetic field results in a measured magnetization signal that is the ensemble average $\langle e^{i\Phi}\rangle$ [24], with $\Phi = \int_0^t g(t')x(t')\,dt'$, where $x(t)$ represents the coordinate of each tagged spin (i.e. walker) in the gradient's direction. Varying the function g makes it possible to highlight diverse properties of small scale fluid motions, provided they satisfy precise hypotheses. This point was the subject of a considerable amount of work [41] assuming that diffusion is normal. Here, we address the case where this assumption is not valid, so that many commonly used theoretical tools become questionable. For instance, [8, 9] path integrals of the form of $\int_0^T u(x(t'))\,dt'$ (i.e. with a kernel, depending on particle position, *a priori* not on time) can be addressed on the basis of variants of the Feynman–Kac equation [42] that significantly differ from the classical version, valid when diffusion is normal. Here, relaxing this assumption, we will focus on gradients $g(t) = a[\delta(t-t_2)-\delta(t-t_1)]$ consisting of two narrow pulses, to code the spins carried by water molecules between two distinct times t_1 and t_2 (with $t_1 < t_2$).

With the two gradient pulses as above, the phase change resulting from the displacement of spins following their own trajectories during time $t > t_2$ is $\Phi = a[x(t_2) - x(t_1)]$. If small scale motions of spin bearers could be represented by a Markov process with independent increments, the ensemble average would also satisfy $\langle e^{i\Phi}\rangle = \int \mathcal{P}(r, t_2 - t_1)e^{iar}\,dr$, with the propagator $\mathcal{P}(r, \Delta t)$ being the probability density that a displacement r occurs during a time interval of duration Δt. This latter propagator is usually calculated using an inverse Fourier transform. With memory effects, using the Markov property becomes hazardous: the existence of a propagator as $\mathcal{P}$ becomes questionable. Thus, we will develop an alternate method.

When the above described magnetic gradient is applied, the magnetization signal $\langle e^{i\Phi}\rangle$ is the mathematical expectation $\langle e^{ia[x(t_2)-x(t_1)]}\rangle$, which sums up the contributions of all walkers in the porous medium. Hence, the functional $\langle e^{ia[x(t_2)-x(t_1)]}\rangle$ of a transport process such as $x(t)$ is worthy of interest in the NMR context. The connection with the (infinite) sequence of the moments of the displacement $x(t_2) - x(t_1)$ is obvious, since we have $\langle e^{ia[x(t_2)-x(t_1)]}\rangle = \Sigma_{n\geq 0}((ia)^n/n!)\langle[x(t_2) - x(t_1)]^n\rangle$. For $Z(t) = t$, i.e. for a process $x(t)$ equal to Brownian motion with a mean velocity, $\langle e^{i\Phi}\rangle$ would be exactly $e^{iav(t_2-t_1)-Da^2(t_2-t_1)}$, since the integral of a Gaussian random variable is also Gaussian. More generally, for processes $x(t)$ obtained from (2) for $\gamma = 1$, $\langle e^{i\Phi}\rangle$ would be $e^{iav(t_2-t_1)/(\Lambda+1)-Da^2(t_2-t_1)/(\Lambda+1)}$. We will see that the long-tailed immobile periods, or equivalently the assumptions made for Z, lead to a different time behavior for $\langle e^{i\Phi}\rangle$. Computing moments of the increments of Z will be essential progress, since Z concentrates all the information concerning the memory effects as well as the statistics of the immobile periods.

The initial position x_0 of a walker is often assumed constant in theoretical works, which corresponds well to the case of a tracer cloud launched at a certain point. However, in NMR experiments, all spin bearing water molecules are accounted for, so that x_0 can be considered as a uniformly distributed random variable, for instance. Addressing functionals of the increment of $x(t)$ in the time interval $[t_1, t_2]$ avoids irrelevant questions concerning x_0.

J. Stat. Mech. (2011) P02006

3. Moments of increments of $Z(t)$ and $x(t)$

Let us first see that moments of the displacements of walkers (i.e. of x) will be deduced almost immediately from those of the increments of $Z(t)$. Then we present the calculation of the moments of $Z(t)$ itself.

3.1. From moments of $Z(t_2) - Z(t_1)$ to moments of $x(t_2) - x(t_1)$

Considering equation (2) we can write

$$\langle [x(t_2) - x(t_1)]^n \rangle = \Sigma_{0\le k\le n} \binom{n}{k} v^k \left\langle [Z(t_2) - Z(t_1)]^k \right\rangle (2D)^{(n-k)/2} \times \left\langle [B(Z(t_2)) - B(Z(t_1))]^{n-k} \right\rangle \tag{6}$$

since $B(Z(t))$ and $Z(t)$ are independent. Moments of the subordinated Brownian motion $B(Z(t))$ have the form of

$$\langle [B(Z(t_2)) - B(Z(t_1))]^n \rangle = \left\langle \int\int_{(z_1,z_2)\in R^{+2}} [B(z_2) - B(z_1)]^n h(z_2, z_1, t_2, t_1)\, \mathrm{d}z_1\, \mathrm{d}z_2 \right\rangle \tag{7}$$

where $h(z_2, z_1, t_2, t_1)$ represents the joint two-times p.d.f. of Z, i.e. $\langle \delta[Z(t_2) - z_2]\delta[Z(t_1) - z_1] \rangle$ [5]. Moreover, for all values of z_1 and z_2 in R^+, moments $\langle [B(z_2) - B(z_1)]^n \rangle$ of odd order n are equal to zero, while moments of even order $2p$ satisfy $\langle [B(z_2) - B(z_1)]^{2p} \rangle = |z_2 - z_1|^p ((2p)!/2^p p!)$ [3]. Hence, the $\langle [B(Z(t_2)) - B(Z(t_1))]^n \rangle$ of odd order n vanish, whereas even order moments satisfy

$$\left\langle [B(Z(t_2)) - B(Z(t_1))]^{2p} \right\rangle = \langle |Z(t_2) - Z(t_1)|^p \rangle \frac{(2p)!}{2^p p!}. \tag{8}$$

Hence, for the increments of $x(t)$, only even values of $n - k$ contribute to $\langle [B(Z(t_2)) - B(Z(t_1))]^{n-k} \rangle$ in (6), and setting $n - k = 2p$ we have

$$\langle [x(t_2) - x(t_1)]^n \rangle = \Sigma_{0\le p\le n/2} \binom{n}{2p} v^{n-2p} \left\langle [Z(t_2) - Z(t_1)]^{n-2p} \right\rangle \times \frac{(2p)!}{p!} D^p \langle |Z(t_2) - Z(t_1)|^p \rangle, \tag{9}$$

with exactly the same link between increments of x_{FFPE} and Z_{FFPE}. Since Z is an increasing process, with $t_2 > t_1$, the absolute value is not necessary in equation (9), and will be discarded.

Thus, in order to determine the moments of the displacement, the remaining task is to compute the moments of $Z(t_2) - Z(t_1)$ (or $Z_{\mathrm{FFPE}}(t_2) - Z_{\mathrm{FFPE}}(t_1)$).

3.2. Moments of $Z(t_2) - Z(t_1)$

Moments of $Z(t_2) - Z(t_1)$ satisfy a general formula of [27], based upon renewal theory [4, 35, 43], and that we will apply, since it holds for the inverses of increasing Lévy processes [44], with or without a drift.

Lévy processes start from 0 and have stationary independent increments; $U(z)$ and $U_{\mathrm{FFPE}}(z)$ are particular cases [30]. Recall that a Lévy time process, positively supported (as $U(z)$ and $U_{\mathrm{FFPE}}(z)$), has a characteristic function (i.e. the Laplace transform of the

J. Stat. Mech. (2011) P02006

p.d.f) of the form of $\mathrm{e}^{-z\psi(\lambda)}$ [27]. For U, the log-characteristic function (in the exponent) is equal to $\psi(\lambda) = \Lambda\lambda^\gamma + \lambda$, whereas it becomes $\psi_{\mathrm{FFPE}}(\lambda) = \Lambda\lambda^\gamma$ for U_{FFPE}. An important tool is the measure $\mathcal{R}$, defined over R^+ by $\mathcal{R}]s,t] = \langle Z(t) - Z(s)\rangle$. As usual in probability theory, the symbol $\mathcal{R}$ also serves for the cumulative distribution function $\mathcal{R}(t) = \langle Z(t)\rangle$ (specifying the arguments makes the difference between measure and function). The Laplace transform of the measure $\mathcal{R}$ is $\int_0^{+\infty} \mathrm{e}^{-\lambda t}\mathcal{R}\{\mathrm{d}t\} = 1/\psi(\lambda)$ [27], where $\{\mathrm{d}t\}$ represents the interval $]t, t + \mathrm{d}t]$. When the measure $\mathcal{R}$ has a density R, its Laplace transform is the Laplace transform of the function R, i.e. $\tilde{R}(\lambda) = 1/\psi(\lambda)$. The paper [27] notes that $\mathcal{R}$ is also the renewal measure of a renewal process (i.e. it counts the average number of points per time interval) [43], and for this reason $\mathcal{R}(t)$ is a renewal function.

Theorem 1 of [27], proved on the basis of this latter point, uses a formula, valid for renewal processes. It states that for $0 < t_1 < t_2$ we have

$$\langle [Z(t_2) - Z(t_1)]^n\rangle = n! \int \cdots \int_{t_1<\theta_1<\theta_2<\cdots<\theta_n<t_2} \mathcal{R}\{\mathrm{d}\theta_n - \theta_{n-1}\} \times \mathcal{R}\{\mathrm{d}\theta_{n-1} - \theta_{n-2}\}\cdots\mathcal{R}\{\mathrm{d}\theta_2 - \theta_1\}\mathcal{R}\{\mathrm{d}\theta_1\} \tag{10}$$

where $\{\mathrm{d}\theta - \theta_0\}$ represents $]\theta - \theta_0, \theta - \theta_0 + \mathrm{d}\theta]$ (i.e. $-\theta_0$ accounts for the translation of amplitude $-\theta_0$). When the measure $\mathcal{R}$ has a density R, the n-fold integral on the right-hand side of equation (10) is

$$\int \cdots \int_{t_1<\theta_1<\theta_2<\cdots<\theta_n<t_2} R(\theta_n - \theta_{n-1})R(\theta_{n-1} - \theta_{n-2})\cdots R(\theta_2 - \theta_1) \times R(\theta_1)\,\mathrm{d}\theta_n\,\mathrm{d}\theta_{n-1}\cdots\mathrm{d}\theta_2\,\mathrm{d}\theta_1,$$

equal to

$$\int_{y_1=0}^{t_2-t_1} R(y_1 + t_1)\,\mathrm{d}y_1 \int_{y_2=y_1}^{t_2-t_1} R(y_2 - y_1)\,\mathrm{d}y_2 \cdots \int_{y_{n-1}=y_{n-2}}^{t_2-t_1} R(y_{n-1} - y_{n-2})\,\mathrm{d}y_{n-1} \times \int_{y_n=y_{n-1}}^{t_2-t_1} R(y_n - y_{n-1})\,\mathrm{d}y_n$$

due to the change of variables $\theta_1 = y_1 + t_1$, $\theta_2 = y_2 + t_1, \ldots, \theta_n = y_n + t_1$. This implies

$$\langle [Z(t_2) - Z(t_1)]^n\rangle = n![R(t + t_1) * R(t) * \cdots * R(t) * \mathcal{R}(t)](t_2 - t_1), \tag{11}$$

where all convolutions correspond to the dumb variable t, while $R(t)*\cdots*R(t)$ represents $n-2$ successive convolutions of R with itself. Since $\mathcal{R}(t) = [R * 1](t)$, this latter equation is equivalent to

$$\langle [Z(t_2) - Z(t_1)]^n\rangle = n![R(t + t_1) * [R^{(n-1)*} * 1](t)](t_2 - t_1), \tag{12}$$

with R^{n*} denoting the n-times iterated convolution of R with itself. With our definition of U we obtain $R(t) = E_{1-\gamma}(-\Lambda t^{1-\gamma})$ with $E_{1-\gamma}$ denoting the Mittag-Leffler function of the order of $1-\gamma$ [45]. For $n = 1$, equation (12) takes the form of

$$\langle [Z(t_2) - Z(t_1)]\rangle = \mathcal{R}(t_2 - t_1) = \mathcal{R}(t_2) - \mathcal{R}(t_1) = \int_{t_1}^{t_2} E_{1-\gamma}(-\Lambda t'^{1-\gamma})\,\mathrm{d}t'.$$

For the variant based upon a zero drift direct subordinator (U_{FFPE}), we have $R_{\mathrm{FFPE}}(t) = \Lambda^{-1}(t^{\gamma-1}/\Gamma(\gamma))$, and $[R_{\mathrm{FFPE}}(t + t_1) * [R_{\mathrm{FFPE}}^{(n-1)*} * 1](t)](t_2 - t_1) =$

$\Lambda^{-n}[((t+t_1)^{\gamma-1}/\Gamma(\gamma)) * (t^{(n-1)\gamma}/\Gamma((n-1)\gamma+1))](t_2-t_1)$, where multiple convolutions reduce to a single one. This implies

$$\langle (Z_{\mathrm{FFPE}}(t_2)-Z_{\mathrm{FFPE}}(t_1))^n\rangle = n!\Lambda^{-n}\left[\frac{t^{(n-1)\gamma}}{\Gamma((n-1)\gamma+1)} * \frac{(t+t_1)^{\gamma-1}}{\Gamma(\gamma)}\right](t_2-t_1), \tag{13}$$

where with $\Lambda = 1$ we obtain $\langle Z_{\mathrm{FFPE}}(t)^n\rangle = n!(t^{n\gamma}/\Gamma(n\gamma+1))$, in agreement with equation (41) of [5]. In this reference, correlations of the form of $\langle Z_{\mathrm{FFPE}}(t_2)Z_{\mathrm{FFPE}}(t_1)\rangle$ were also computed. Of course they satisfy

$$\langle Z_{\mathrm{FFPE}}(t_2)Z_{\mathrm{FFPE}}(t_1)\rangle = \tfrac{1}{2}[\langle Z_{\mathrm{FFPE}}(t_1)^2\rangle + \langle Z_{\mathrm{FFPE}}(t_2)^2\rangle - \langle [Z_{\mathrm{FFPE}}(t_2)-Z_{\mathrm{FFPE}}(t_1)]^2\rangle],$$

and on the right-hand side we have

$$\frac{t_1^{2\gamma}+t_2^{2\gamma}}{\Gamma(2\gamma+1)} - \frac{[t^\gamma * (t+t_1)^{\gamma-1}]\,(t_2-t_1)}{\Gamma(\gamma)\Gamma(\gamma+1)}.$$

Since

$$\frac{[t^\gamma * (t+t_1)^{\gamma-1}]\,(t_2-t_1)}{\Gamma(\gamma)\Gamma(\gamma+1)} = \int_0^{t_2}\frac{\theta^{\gamma-1}(t_2-\theta)^\gamma}{\Gamma(\gamma)\Gamma(\gamma+1)}\,\mathrm{d}\theta - \int_0^{t_1}\frac{\theta^{\gamma-1}(t_2-\theta)^\gamma}{\Gamma(\gamma)\Gamma(\gamma+1)}\,\mathrm{d}\theta,$$

where in $\int_0^{t_2}(\theta^{\gamma-1}(t_2-\theta)^\gamma/\Gamma(\gamma)\Gamma(\gamma+1))\,\mathrm{d}\theta = t_2^{2\gamma}\int_0^1(\Theta^{\gamma-1}(1-\Theta)^\gamma/\Gamma(\gamma)\Gamma(\gamma+1))\,\mathrm{d}\Theta$ we recognize the Bernoulli beta function $\int_0^1 \mathrm{d}\Theta\,\Theta^{\gamma-1}(1-\Theta)^\gamma = (\Gamma(\gamma+1)\Gamma(\gamma)/\Gamma(2\gamma+1))$, we arrive at

$$\langle Z_{\mathrm{FFPE}}(t_2)Z_{\mathrm{FFPE}}(t_1)\rangle = \frac{t_1^{2\gamma}}{\Gamma(2\gamma+1)} + \frac{1}{\Gamma(\gamma+1)\Gamma(\gamma)}\int_0^{t_1}\theta^{\gamma-1}(t_2-\theta)^\gamma\,\mathrm{d}\theta,$$

which is equation (B2) of [5] for $t_2 > t_1$.

Whereas the moments of the increments of Z_{FFPE} have a relatively simple expression, equation (12) involves convolutions of functions, which are less common. Therefore, it will be really useful if we can compute the iterated convolutions R^{n*} numerically. The non-local operator $(\mathrm{Id}+\Lambda I_{0,+}^{1-\gamma})^{-1}$, which appeared in equation (4) and determines the fraction of mobile particles within the fractal MIM context [31, 32], will help in achieving this task.

3.3. Iterated convolutions of kernel $R(t)$, and operator $(\mathrm{Id}+\Lambda I_{0,+}^{1-\gamma})^{-1}$

In $\psi(\lambda) = \lambda(1+\Lambda\lambda^{\gamma-1})$ we immediately recognize the Laplace symbol $1+\Lambda\lambda^{\gamma-1}$ of operator $\mathrm{Id}+\Lambda I_{0,+}^{1-\gamma}$, according to appendix. Hence, in $\tilde{R}(\lambda) = 1/\psi(\lambda)$ we have the Laplace symbol of $(\mathrm{Id}+\Lambda I_{0,+}^{1-\gamma})^{-1}$, multiplied by that of the constant function 1. Therefore $R^{n*}*1$, whose Laplace transform is $(1/\lambda^{n+1})(1/(1+\Lambda\lambda^{\gamma-1})^n)$, is also equal to $(\mathrm{Id}+\Lambda I_{0,+}^{1-\gamma})^{-n}(t^n/n!)$. This implies $n![R^{(n-1)*}*1](t) = n(\mathrm{Id}+\Lambda I_{0,+}^{1-\gamma})^{-(n-1)}(t^{n-1})$, and the following proposition is proved.

Proposition 1. *For $n>0$, the process $Z(t)$ defined by (3) satisfies*

$$\langle [Z(t_2)-Z(t_1)]^n\rangle = n!\left[R(t+t_1) * (\mathrm{Id}+\Lambda I_{0,+}^{1-\gamma})^{-(n-1)}\left(\frac{t^{n-1}}{(n-1)!}\right)\right](t_2-t_1). \tag{14}$$

J. Stat. Mech. (2011) P02006

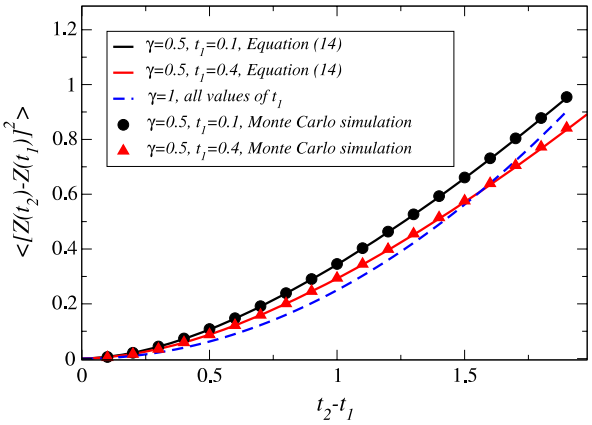

Figure 4. The second order moment $\langle [Z(t_2) - Z(t_1)]^2 \rangle$ for $\gamma = 0.5$, $\Lambda = 1$, and two values of t_1. Full lines represent equation (14), symbols were computed from the random walk $x^\tau(t)$ by setting $v = 1$ and $D = 0$, with 15 000 walkers and $\tau = 0.01$. The two values of t_1 give different results for $\gamma = 0.5$, but not for $\gamma = 1$ (dashed line): then, the memory effects reduce to uniform retardation.

On the right-hand side of equation (14), we have the convolution of two functions. The first one is the Mittag-Leffler type function $R(t + t_1)$, in general computed upon inverting the Laplace transform, which needs integrating over an infinite interval. The second one is defined by iterating the mapping $(\mathrm{Id} + \Lambda I_{0,+}^{1-\gamma})^{-1}$. In fact, both functions can be easily computed upon using a numerical method described in [31] for this latter mapping.

The method consists in noticing that the mapping $\mathrm{Id} + \Lambda I_{0,+}^{1-\gamma}$ is easily discretized on the base of a trapezoidal scheme for the fractional integral [46]. From this scheme we deduce an approximation for $(\mathrm{Id} + \Lambda I_{0,+}^{1-\gamma})^{-1}$ upon inverting the triangular matrix that represents $\mathrm{Id} + \Lambda I_{0,+}^{1-\gamma}$ [31]. This method allowed us to rapidly compute the Mittag-Leffler type function $R = (\mathrm{Id} + \Lambda I_{0,+}^{1-\gamma})^{-1}(1)$. It also applies to the discretization of $(\mathrm{Id} + \Lambda I_{0,+}^{1-\gamma})^{-n} = (\mathrm{Id} + \Sigma_{k=1}^{n} \binom{n}{k} \Lambda^k I_{0,+}^{k(1-\gamma)})^{-1}$, which makes the computation of all one-time moments, of all orders, very quick.

Figure 4 illustrates the second order moment $\langle [Z(t_2) - Z(t_1)]^2 \rangle$, computed according to this method as a function of $t_2 - t_1$ for two fixed values of t_1. Comparisons against a Monte Carlo simulation of a random walk approximation of $Z(t)$ are also displayed. The excellent agreement represents a direct check of (14), and of the above numerical method. For $\gamma < 1$, the second moment of $Z(t_2) - Z(t_1)$ depends on t_1 and not only on $t_2 - t_1$. In the limiting case $\gamma = 1$, differently, the memory effects take the trivial form of $(Z(t) = t/(1 + \Lambda))$, since then $U(z)$ becomes deterministic (namely equal to $(1 + \Lambda)z$).

Thus, as mentioned before, moments of $x(t_2) - x(t_1)$ can be deduced from those of $Z(t_2) - Z(t_1)$.

3.4. Moments of $x(t_2) - x(t_1)$

Combining equations (9) and (14) yields the moments of the displacement $x(t_2) - x(t_1)$. Second order moments behave according to

$$\left\langle [x(t_2) - x(t_1)]^2 \right\rangle = 2v^2 [R(t + t_1) * \mathcal{R}(t)](t_2 - t_1) + 2D\mathcal{R}(t_2 - t_1). \qquad (15)$$

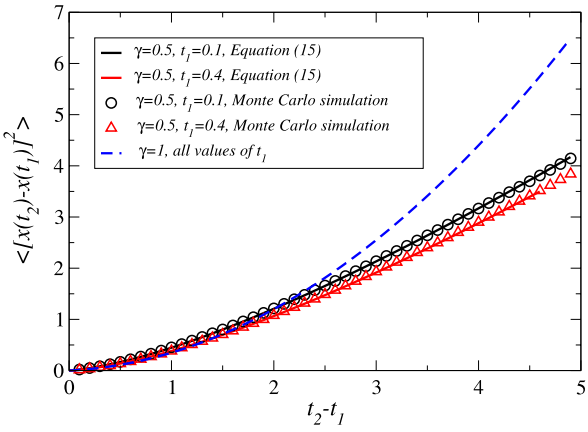

Figure 5. The second order moment $\langle [x(t_2) - x(t_1)]^2 \rangle$ for $\gamma = 0.5$, $\Lambda = 1$, $v = 1$, $D = 0.1$, and two values of t_1. Full lines represent equation (15), symbols were computed from the random walk $x^\tau(t)$, with 15 000 walkers and $\tau = 0.01$. For $\gamma = 1$ (dashed line), the value of t_1 does not influence the value of $\langle [x(t_2) - x(t_1)]^2 \rangle$, whereas for $\gamma = 0.5$ it does.

The comparison against Monte Carlo simulations is represented in figure 5, and we (again) notice that the moments depend on t_1, not only on $t_2 - t_1$, for $\gamma < 1$. They grow more slowly when γ is decreased (except at small values of $t_2 - t_1$).

Using the mapping $(\mathrm{Id} + \Lambda I_{0,+}^{1-\gamma})^{-1}$ also provides closed form expressions for the functionals $\langle \mathrm{e}^{\eta[Z(t_2) - Z(t_1)]} \rangle$ and $\langle \mathrm{e}^{\eta[x(t_2) - x(t_1)]} \rangle$.

4. The mathematical expectation of $\mathrm{e}^{\eta[x(t_2) - x(t_1)]}$

Similar to what we have seen for moments, computing $\langle \mathrm{e}^{\eta[Z(t_2) - Z(t_1)]} \rangle$ is the main step toward $\langle \mathrm{e}^{\eta[x(t_2) - x(t_1)]} \rangle$.

4.1. Mathematical expectation of $\mathrm{e}^{\eta[Z(t_2) - Z(t_1)]}$

Since equation (14) computes the mathematical expectations of all items present in the expansion of $\mathrm{e}^{\eta[Z(t_2) - Z(t_1)]}$, summing up the series of the general term $\langle [Z(t_2) - Z(t_1)]^n \rangle (\eta^n / n!)$ leads to an expression for $\langle \mathrm{e}^{\eta[Z(t_2) - Z(t_1)]} \rangle$. We write the sum in a closed form, as a Neumann series can be recognized. To this end, we will take advantage of the fact that the function $(t^{n-1}/(n-1)!)$ (on the right-hand side of equation (14)) is obtained by applying the operator $I_{0,+}^{n-1}$ to the constant function 1, so that this expression is

$$\langle \mathrm{e}^{\eta[Z(t_2) - Z(t_1)]} \rangle = 1 + \eta \left[R(t + t_1) * \left[\Sigma_{n \geq 0} \eta^n (\mathrm{Id} + \Lambda I_{0,+}^{1-\gamma})^{-n} I_{0,+}^n (1) \right](t) \right] (t_2 - t_1). \tag{16}$$

On the right-hand side we have the series $\Sigma_{n \geq 0} \eta^n (\mathrm{Id} + \Lambda I_{0,+}^{1-\gamma})^{-n} I_{0,+}^n (1)$, whose generic term is a function of t, obtained by applying successively the mappings $I_{0,+}^n$ and $(\mathrm{Id} + \Lambda I_{0,+}^{1-\gamma})^{-n}$ to the constant function 1. We will see that this is equivalent to applying (for all values of n) the nth power of some operator.

A preliminary point is that $(\mathrm{Id} + \Lambda I_{0,+}^{1-\gamma})^{-1}$ and $I_{0,+}^1$ commute, due to the fact that the mapping $(\mathrm{Id} + \Lambda I_{0,+}^{1-\gamma})^{-1}$ is the inverse of $(\mathrm{Id} + \Lambda I_{0,+}^{1-\gamma})$, not only a left inverse as $\Lambda^{-1} D_{0,+}^{1-\gamma}$

J. Stat. Mech. (2011) P02006

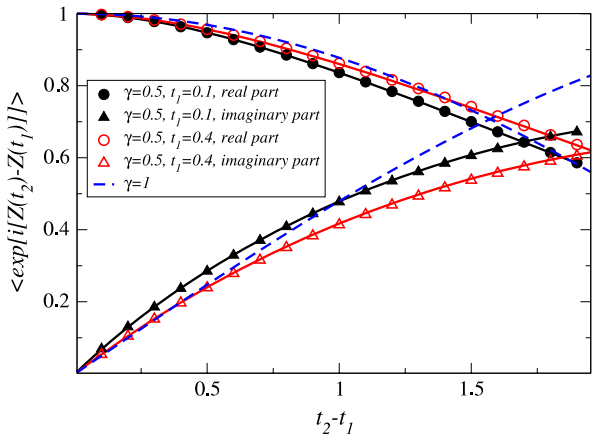

Figure 6. The mathematical expectation of $e^{i[Z(t_2)-Z(t_1)]}$. Full lines represent the real and imaginary part of $\langle e^{i[Z(t_2)-Z(t_1)]}\rangle$ for $\gamma = 0.5$ and $\Lambda = 1$, computed from (18), compared with Monte Carlo simulation (symbols). Two values of t_1 are displayed: they influence the value of $\langle e^{i[Z(t_2)-Z(t_1)]}\rangle$ for $\gamma < 1$, whereas in the limiting case $\gamma = 1$, $Z(t) = t/(\Lambda + 1)$ implies that $\langle e^{i[Z(t_2)-Z(t_1)]}\rangle = e^{i(t_2-t_1)/(\Lambda+1)}$ does not depend on t_1 (dashed line).

is for $\Lambda I_{0,+}^{1-\gamma}$ [31]. This, in turn, is because the Neumann series $\Sigma_{n\geq 0}(-\Lambda I_{0,+}^{1-\gamma})^n$ converge in $X_\chi = \{f/\|f\|_\chi < \infty\}$ with $\|f\|_\chi = \|e^{-\chi t} f(t)\|_{L^2[0,T]}$ for any positive χ, because lemma 3 of [47] states that $\|I_{0,+}^\alpha g\|_\chi \leq \chi^{-1}\|g\|_\chi$ for every g in X_χ. Hence, mappings such as the $I_{0,+}^\alpha$ are contracting in X_χ, provided we take $\chi > 1$. Consequently $(\mathrm{Id} + \Lambda I_{0,+}^{1-\gamma})^{-1}$ commutes with the integral $I_{0,+}^1$, since integrals of positive orders commute.

Now, on the right-hand side of (16) we have the Neumann series $\Sigma_{n\geq 0}\eta^n[(\mathrm{Id} + \Lambda I_{0,+}^{1-\gamma})^{-1} I_{0,+}^1]^n(1)$, whose sum is $[\mathrm{Id} - \eta(\mathrm{Id} + \Lambda I_{0,+}^{1-\gamma})^{-1} I_{0,+}^1]^{-1}(1)$, provided this sum exists. This latter point is easily checked upon noticing that $(\mathrm{Id} + \Lambda I_{0,+}^{1-\gamma})^{-1} I_{0,+}^1$ is a convolution, whose kernel R is positively valued. Consequently, the mapping $(\mathrm{Id} + \Lambda I_{0,+}^{1-\gamma})^{-1} I_{0,+}^1$ is sign preserving: for each non-negative function g, $f = (\mathrm{Id} + \Lambda I_{0,+}^{1-\gamma})^{-1} I_{0,+}^1 g$ is also non-negative. For such functions g in X_χ with $\chi > 1$, this implies $\|f\|_\chi \leq \|g\|_\chi$. Hence the series $\Sigma_{n\geq 0}\eta^n[(\mathrm{Id} + \Lambda I_{0,+}^{1-\gamma})^{-1} I_{0,+}^1]^n(1)$ converge in X_χ and the following proposition is proved.

Proposition 2. *For Z defined by (3) we have*

$$\left\langle e^{\eta[Z(t_2)-Z(t_1)]}\right\rangle = 1 + \eta[R(t + t_1) * [\mathrm{Id} - \eta(\mathrm{Id} + \Lambda I_{0,+}^{1-\gamma}]^{-1} I_{0,+}^1)^{-1}(1)](t_2 - t_1). \tag{17}$$

The mapping $[\mathrm{Id} - \eta(\mathrm{Id} + \Lambda I_{0,+}^{1-\gamma}]^{-1} I_{0,+}^1)$, to be inverted on the right-hand side of this equation, is equal to $(\mathrm{Id} + \Lambda I_{0,+}^{1-\gamma})^{-1}(\mathrm{Id} + \Lambda I_{0,+}^{1-\gamma} - \eta I_{0,+}^1)$. Hence, the inverse is $(\mathrm{Id} + \Lambda I_{0,+}^{1-\gamma} - \eta I_{0,+}^1)^{-1}(\mathrm{Id} + \Lambda I_{0,+}^{1-\gamma})$, whose first item was discretized by using the same method as for $(\mathrm{Id} + \Lambda I_{0,+}^{1-\gamma})^{-1}$ itself:

$$\left\langle e^{\eta[Z(t_2)-Z(t_1)]}\right\rangle = 1 + \eta[R(t + t_1) * (\mathrm{Id} + \Lambda I_{0,+}^{1-\gamma} - \eta I_{0,+}^1)^{-1}(\mathrm{Id} + \Lambda I_{0,+}^{1-\gamma})(1)](t_2 - t_1). \tag{18}$$

As it was done for moments, the right-hand side was successfully compared with Monte Carlo simulations, illustrated in figure 6. Here again, the result depends on t_1 and not only on $t_2 - t_1$, except for $\gamma = 1$.

J. Stat. Mech. (2011) P02006

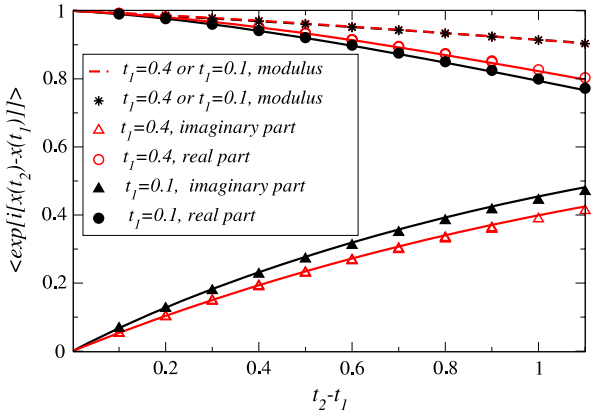

Figure 7. Expectation of the exponential of the displacement $e^{ia[x(t_2)-x(t_1)]}$. For $\gamma = 0.5$, $D = 0.1$, $\Lambda = 1$, $v = 1$ and $a = 1$, the real and imaginary parts of $\langle e^{ia[x(t_2)-x(t_1)]}\rangle$ were computed from equation (21) (full lines), and compared with a Monte Carlo simulation (symbols) with $\tau = 0.01$. For the two values of t_1, represented here, the complete (complex) signal shows visible differences. In counterpart, the modulus (dashed lines) of the signal is much less influenced than the phase.

It now remains to conclude with $\langle e^{\eta[x(t_2)-x(t_1)]}\rangle$ itself, for all values of η and especially for purely imaginary values as measured by NMR.

4.2. Mathematical expectation of $e^{\eta[x(t_2)-x(t_1)]}$

Since $B(Z(t))$ and $Z(t)$ are independent, the observable $\langle e^{ia[x(t_2)-x(t_1)]}\rangle$ satisfies

$$\langle e^{ia[x(t_2)-x(t_1)]}\rangle = \langle e^{iva[Z(t_2)-Z(t_1)]}\rangle\langle e^{ia\sqrt{2D}[B(Z(t_2))-B(Z(t_1))]}\rangle, \tag{19}$$

where, due to (8), we have

$$\langle e^{ia\sqrt{2D}[B(Z(t_2))-B(Z(t_1))]}\rangle = \Sigma_{n\geq 0}\frac{(-a^2D)^n}{n!}\langle[Z(t_2)-Z(t_1)]^n)\rangle = \langle e^{-a^2D[Z(t_2)-Z(t_1)]}\rangle \tag{20}$$

for $t_2 > t_1$.

Upon inserting equation (18) into equations (19) and (20), with $\eta = a^2D$ we obtain

$$\begin{aligned}\left\langle e^{ia[x(t_2)-x(t_1)]}\right\rangle = [1 + iav[E_{1-\gamma}(-\Lambda(t+t_1)^{1-\gamma}) * (\mathrm{Id} + \Lambda I_{0,+}^{1-\gamma} - iavI_{0,+}^{1})^{-1}(\mathrm{Id} + \Lambda I_{0,+}^{1-\gamma})(1)]\\ \times (t_2 - t_1)][1 - \eta[E_{1-\gamma}(-\Lambda(t+t_1)^{1-\gamma}) * (\mathrm{Id} + \Lambda I_{0,+}^{1-\gamma} + \eta I_{0,+}^{1})^{-1}\\ \times (\mathrm{Id} + \Lambda I_{0,+}^{1-\gamma})(1)](t_2 - t_1)]\end{aligned} \tag{21}$$

represented in figure 7, where it is compared against Monte Carlo simulations.

In the FFPE case, for all values of η the mathematical expectation of the exponential of the increments of the inverse subordinator Z_{FFPE} is

$$\begin{aligned}\left\langle e^{\eta[Z_{\mathrm{FFPE}}(t_2)-Z_{\mathrm{FFPE}}(t_1)]}\right\rangle &= 1 + \frac{\eta}{\Lambda}\left[R(t+t_1) * \Sigma_{n\geq 0}\left(\frac{\eta}{\Lambda}\right)^n \frac{t^{n\gamma}}{\Gamma(n\gamma+1)}\right](t_2 - t_1)\\ &= 1 + \frac{\eta}{\Lambda}\left[\frac{(t+t_1)^{\gamma-1}}{\Gamma(\gamma)} * E_\gamma\left(\frac{t^\gamma\eta}{\Lambda}\right)\right](t_2 - t_1).\end{aligned} \tag{22}$$

J. Stat. Mech. (2011) P02006

Setting $t_1 = 0$, $\Lambda = 1$, $\eta = -a^2 D$ and $v = 0$ we obtain for the characteristic function of the subordinated Brownian motion $\sqrt{2D}B(Z_{\mathrm{FFPE}}(t))$,

$$\langle \mathrm{e}^{\mathrm{i}a\sqrt{2D}B(Z_{\mathrm{FFPE}}(t))}\rangle = \langle \mathrm{e}^{-a^2 D Z_{\mathrm{FFPE}}(t)}\rangle = 1 - a^2 D I^{\gamma}_{0,+} E_{\gamma}(-t^{\gamma} a^2 D),$$

whose Laplace transform is $(1/\lambda) - (a^2 D\lambda^{-\gamma}/(\lambda + a^2 D\lambda^{1-\gamma})) = 1/(\lambda + a^2 D\lambda^{1-\gamma})$, so that we retrieve equation (49) of [15], namely $\langle \mathrm{e}^{\mathrm{i}a\sqrt{2D}B(Z_{\mathrm{FFPE}}(t))}\rangle = E_{\gamma}(-t^{\gamma} a^2 D)$.

5. Conclusion and perspectives

The increments of subordinated Brownian motions were addressed, assuming inverse Lévy subordinators with or without drift. In both cases, exact expressions were given to moments and characteristic functions (of the increments). In the FFPE case where the direct subordinator has a drift equal to zero, all moments are convolutions involving power functions, in continuation with previous results of [5]. The characteristic function is the convolution of a power, with a function of Mittag-Leffler type.

The case where the direct subordinator involves a drift corresponds to stochastic models, used by several authors to describe mass transport in porous media showing memory effects. NMR is a powerful tool to investigate this type of transport. Indeed, a frequently used approach precisely records an electromagnetic signal that is the characteristic function of fluid particle displacement, therefore motivating our interest. However, moments and characteristic functions of walker displacements $x(t_2) - x(t_1)$, here represented by increments of a subordinated Brownian motion, have then more complex expressions than in the FFPE case: they involve the inverses of operators, equal to the sum of identity, plus fractional integrals w.r.t. time. A discretization method had been previously designed for such operators, within the fractal MIM context.

Thus, the NMR response was calculated using the model detailed in section 4 (especially formula (21) for the case corresponding to the fractal MIM) and Monte Carlo simulations of the underlying process. Excellent agreement was found between the two methods, providing a convincing validation of our calculations. The stochastic model, studied here, encompasses Brownian motion and MIM as limiting cases, and is labeled by a key parameter representing the memory effect, namely the exponent of the Lévy law in equations (1) and in the stochastic process U.

We can already state from numerical results presented here, that the signal should depend, although weakly (particularly in the case of the modulus), not only on the time step $t_2 - t_1$ but also on the past history of the experiment. The availability of an expression for the NMR signal, directly linked to model parameters, avoids the calculation of propagators by Fourier transforms, which might not be strictly valid in the case of non-Markovian processes.

On the basis of formula (21), using both numerical simulation and the mathematical expression, we can expect extracting the parameter γ from experimental NMR data, along with the diffusivity D and the scale factor Λ, at least in devices whose initial instant is well defined. To this end, we will use the fact that the above parameters do not affect the same part of the displacement curves. For example, the values of D can be determined at short time difference, before memory effects become important. Figure 7 indicates that the influence of t_1 on the modulus of the signal is very small, when t_1 remains moderate, and this can be used. We also will vary a, t_1, t_2 and look for values of Λ and γ such as to

J. Stat. Mech. (2011) P02006

minimize the distance between the measured signal and the mathematical expression (21). Finally, another possibility is to exploit the information given in the transverse direction of the flow not affected by the average velocity, as the applied field gradients can be set in any direction.

However, formulas ((18) and (21)) were obtained without accounting for boundary conditions, or for the fact that some particles leave the device during the experiment and are replaced by fresh ones. Estimating the resulting error will be the duty of further work. Extending the results of [8, 9] and [48] will certainly be necessary for that.

Acknowledgments

This work was supported by Agence Nationale de la Recherche (ANR project ANR-09-SYSC-015) and by the Groupement MoMas (Modélisation Mathématique et Simulations numériques liées aux problèmes de gestion des déchets nucléaires).

Appendix. Fractional integrals and derivatives

The fractional integral $I^{\alpha}_{0,+}f$ of order $\alpha > 0$ is

$$I^{\alpha}_{0,+}f(t) = \frac{1}{\Gamma(\alpha)} \int_0^t (t-t')^{\alpha-1} f(t')\, \mathrm{d}t', \tag{A.1}$$

which generalizes the usual multiple integrals to non-integer order [39]. Observe that $I^{\alpha}_{0,+}$ is bounded in $L^p[0,T]$ for $1 \leq p \leq \infty$ [39], and that it is a convolution, of kernel $t^{\alpha-1}/\Gamma(\alpha)$. In Laplace variables ($\lambda$) the symbol of $I^{\alpha}_{0,+}$ is $\lambda^{-\alpha}$. The Riemann–Liouville derivative $D^{\alpha}_{0,+}$ is the left inverse of the integral: for every suitable function f, we have $D^{\alpha}_{0,+} I^{\alpha}_{0,+} f = f$. We also have $I^{\alpha}_{0,+} I^{\beta}_{0,+} f = I^{\alpha+\beta}_{0,+} f$.

References

[1] Majumdar S N, 2005 *Curr. Sci.* **89** 2076
[2] Billingsley P, 1999 *Convergence of Probability Measures* (*Wiley Series in Probability and Statistics*) 2nd edn (New York: Wiley)
[3] Oksendahl B, 2003 *Stochastic Differential Equations: An Introduction with Applications* 6th edn (Berlin: Springer)
[4] Godrèche C and Luck J M, 2001 *J. Stat. Phys.* **104** 489
[5] Baule A and Friedrich R, 2005 *Phys. Rev.* E **71** 026101
[6] Baule A and Friedrich R, 2007 *Europhys. Lett.* **79** 6004
[7] Barkai E and Sokolov I M, 2007 *J. Stat. Mech.* P08001
[8] Turgeman L, Carmi S and Barkai E, 2009 *Phys. Rev. Lett.* **103** 190201
[9] Carmi S, Turgeman L and Barkai E, 2010 *J. Stat. Phys.* **141** 1071
[10] Bromly M and Hinz C, 2004 *Water Resour. Res.* **40** W07402
[11] Zhang Y, Benson D A and Bauemer B, 2008 *Water Resour.* **44** W05404
[12] Schumer R, Benson D A, Meerschaert M M and Bauemer B, 2003 *Water Resour. Res.* **39** 1296
[13] Benson D A and Meerschaert M M, 2009 *Adv. Water Resour.* **32** 532
[14] Zaslavsky G, 1994 *Physica* D **76** 110
[15] Metzler R and Klafter J, 2000 *Phys. Rep.* **339** 1
[16] Metzler R and Klafter J, 2004 *J. Phys. A: Math. Gen.* **37** R161
[17] Barkai E, Metzler R and Klafter J, 2000 *Phys. Rev.* E **61** 132
[18] Barkai E, 2001 *Phys. Rev.* E **63** 046118
[19] Magdziarz M, Weron A and Weron K, 2007 *Phys. Rev.* E **75** 016708
[20] Magdziarz M, Weron A and Klafter J, 2008 *Phys. Rev. Lett.* **101** 210601
[21] Magdziarz M, 2009 *J. Stat. Phys.* **135** 763

J. Stat. Mech. (2011) P02006

[22] Weron A, Magdziarz M and Weron K, 2008 *Phys. Rev.* E **77** 036704
[23] Berkowitz B, Cortis A, Dentz M and Scher H, 2006 *Rev. Geophys.* **44** RG2003
[24] Callaghan P T, 1991 *Principles of Nuclear Magnetic Resonance Microscopy* (Oxford: Clarendon)
[25] Sheven U M and Sen P, 2002 *Phys. Rev. Lett.* **89** 254501
[26] Han S-I, Stapf S and Blümich B, 2000 *J. Magn. Reson.* **146** 169
[27] Lageras A N, 2005 *J. Appl. Probab.* **42** 1134
[28] Van Genuchten M T and Wierenga P J, 1976 *Soil. Sci. Soc. Am. J.* **33** 473
[29] Haggerty R and Gorelick S M, 1995 *Water Resour. Res.* **31** 2383
[30] Meerschaert M M and Scheffler H P, 2004 *J. Appl. Probab.* **41** 623
[31] Maryshev B, Joelson M, Lyubimov D, Lyubimova T and Néel M C, 2009 *J. Phys. A: Math. Theor.* **42** 115001
[32] Néel M C, Zoia A and Joelson M, 2009 *Phys. Rev.* E **80** 056301
[33] Gnedenko B V and Kolmogorov A N, 1968 *Limit Distributions for Sums of Independent Variables* (Reading, MA: Addison-Wesley)
[34] Lévy P, 1937 *Théorie de l'addition des Variables Aléatoires* (Paris: Gauthier-Villars)
[35] Feller W, 1970 *An Introduction to Probability Theory and its Applications* vol II (New York: Wiley)
[36] Gorenflo R, Mainardi F and Vivoli A, 2007 *Chaos Solitons Fractals* **34** 87
[37] Meerschaert M M and Scheffler H P, 2000 *Limit Distributions for Sums of Independent Random Vectors* (*Heavy Tails in Theory and Practice*) (New York: Wiley)
[38] Piryatinska A, Saichev A I and Woyczynski W A, 2005 *Physica* A **349** 375
[39] Samko S G, Kilbas A A and Marichev O I, 1993 *Fractional Integrals and Derivatives: Theory and Applications* (New York: Gordon and Breach)
[40] Mainardi F, *Fractional calculus: some basic problems in countinuum and statistical mechanics*, 1997 *Fractals and Fractional Calculus in Continuum Mechanics* (*CISM Courses and Lectures* vol 378) ed A Carpinteri and F Mainardi (New York: Springer) pp 291–348
[41] Grebenkov D S, 2007 *Rev. Mod. Phys.* **79** 1077
[42] Kac M, 1949 *Trans. Am. Math. Soc.* **65** 1
[43] Daley D J and Vere-Jones D, 2005 *An Introduction to The Theory of Point Processes* (*Probability and its Applications*) 3rd edn (Berlin: Springer)
[44] Sato K-I, 1999 *Lévy Processes and Infinitely Divisible Distributions* (*Cambridge Studies in Advanced Mathematics* vol 68) (Cambridge: Cambridge University Press)
[45] Mainardi F and Gorenflo R, 2000 *J. Comput. Appl. Math.* **118** 283
[46] Diethelm K, Ford N J, Freed A D and Luchko Y, 2005 *Comput. Methods Appl. Mech. Eng.* **194** 543
[47] Gorenflo R, Iskenderov A and Yamamoto R, *On the regularization of linear Abel-type integral equations of first kind with Hölder-continuous kernels*, 1997 preprint available on http://www.math.fu-berlin.de
[48] Grebenkov D S, 2007 *Phys. Rev.* E **76** 041139

J. Stat. Mech. (2011) P02006